Polyhedron 28 (2009) 2287–2293

Contents lists available at ScienceDirect

Polyhedron

journal homepage: www.elsevier.com/locate/poly

Crystal structures of (azido)(pentamethylcyclopentadienyl)iridium(III) complexes containing various types of bidentate ligands

Takayoshi Suzuki [a,b,*], Mai Kotera [b], Asuka Takayama [a], Masaaki Kojima [a]

[a] Department of Chemistry, Faculty of Science, Okayama University, Okayama 700-8530, Japan
[b] Department of Chemistry, Graduate School of Science, Osaka University, Toyonaka 560-0043, Japan

ARTICLE INFO

Article history:
Received 16 January 2009
Accepted 14 April 2009
Available online 21 April 2009

Keywords:
Iridium(III) azido complexes
Crystal structures
8-Quinolylphosphine
2-Pyridylphosphine
2-(2-Pyridyl)benzimidazolate

ABSTRACT

Several (azido)iridium(III) complexes having a pentamethylcyclopentadienyl (Cp^*) group, $[Cp^*Ir(N_3)_2(Ph_2Ppy\text{-}\kappa P)]$ (**1**: Ph_2Ppy = 2-diphenylphosphinopyridine), $[Cp^*Ir(N_3)(Ph_2Ppy\text{-}\kappa P,\kappa N)]CF_3SO_3$ (**2**), $[Cp^*Ir(N_3)(dmpm)]PF_6$ (**3**: dmpm = bis(dimethylphosphino)methane), $[Cp^*Ir(N_3)(Ph_2Pqn)]PF_6{\cdot}CH_3OH$ (**4**·CH_3OH: Ph_2Pqn = 8-diphenylphosphinoquinoline), and $[Cp^*Ir(N_3)(pybim)]$ (**5**: Hpybim = 2-(2-pyridyl)benzimidazole) have been prepared and their crystal structures have been analyzed by X-ray diffraction. In complex **1**, the Ph_2Ppy ligand is only coordinated via the P atom (-κP), while in **2** it acts as a bidentate ligand through the P and N atoms (-$\kappa P,\kappa N$) to form a four-membered chelate ring. Comparing the structural parameters of the chelate ring in **2** with those of a similar five-membered chelate ring formed by Ph_2Pqn in **4**, it became apparent that the angular distortion in the Ph_2Ppy-$\kappa P,\kappa N$ ring was remarkable, although the Ir–P and Ir–N bonds in the Ph_2Ppy-$\kappa P,\kappa N$ ring were not elongated very much from the corresponding bonds in the Ph_2Pqn-$\kappa P,\kappa N$ ring. In the pybim complex **5**, the five-membered chelate ring was coplanar with the pyridine and benzimidazolyl rings. With the related (azido)iridium(III) complexes analyzed previously, comparison of the structural parameters of the Ir–N_3 moiety in $[Cp^*Ir^{III}(N_3)(L\text{–}L')]^{+/0}$ complexes reveals an anomalous feature of the 2,2′-bipyridyl (bpy) complex, $[Cp^*Ir(N_3)(bpy)]PF_6$.

1. Introduction

Recently, the investigation of transition-metal azido complexes has been revived because they often show interesting chemical reactivities and physical properties [1–4]. For example, photolysis of some azido complexes results in higher-valent metal nitrido complexes, which have the potential for further nitrogen-atom (or imino-group) transfer reactions [2]. The *crick* reactions of azido complexes with nitriles or alkynes via 1,3-dipolar cycloaddition, which affords the corresponding tetrazolato or triazolato complexes, are also attractive for the creation of new functional compounds [3]. Furthermore, the azido-bridged dinuclear complexes or cluster compounds are of current interest in studies of supramolecular architecture and the development of molecular magnetic materials [4]. We have also investigated the photochemical reactivities of (azido)iridium(III) complexes with a $Cp^*Ir^{III}(N_3)$ ($Cp^* = \eta^5\text{-}C_5Me_5$) fragment, and found a novel nitrogen-atom insertion reaction on photolysis of $[Cp^*Ir(N_3)(R_2dtc$, 2-Spy, or 2-Sqn)] (R_2dtc^- = *N,N*-dialkyldithiocarbamate; 2-Spy^- = 2-pyridinethiolate; 2-Sqn^- = 2-quinolinethiolate) complexes (Scheme 1) [5–7]. This interesting reaction seems to be attributable to the highly strained chelate ring and the stability of the Ir–S bond of the above dithiocarbamato or thiolato ligands. On the other hand, it is also known that some Cp^*Ir^{III} complexes having phosphines or imidazolates often exhibit interesting structural features and novel reactivities [8–11]. Therefore, the related $Cp^*Ir^{III}(N_3)$ complexes bearing 2-diphenylphosphinopyridine (Ph_2Ppy), 8-diphenylphosphinoquinoline (Ph_2Pqn), bis(diphenyl- or dimethylphosphino)methane (dppm or dmpm), as well as 2-(2-pyridyl)benzimidazolate ($pybim^-$) (L–L′: Scheme 2) may be possible candidates for similar or other fascinating reactions. Here, we have prepared such complexes of $[Cp^*Ir^{III}(N_3)(L\text{–}L')]^{+/0}$, and their molecular structures and chemical reactivities were compared, together with the analogous complexes characterized previously in our group [5,7,12,13].

2. Experimental

2.1. Preparation of complexes

The diazidoiridium(III) complex, $[Cp^*Ir(N_3)_2]_2$ [12], and the phosphines, Ph_2Ppy [14] and Ph_2Pqn [15], were prepared by the literature methods. The ligands, dmpm and 2-(pyridyl)benzimidazole (Hpybim), were purchased from Aldrich Co. Ltd.

* Corresponding author. Address: Department of Chemistry, Faculty of Science, Okayama University, Okayama 700-8530, Japan. Tel./fax: +81 86 251 7900.
E-mail address: suzuki@cc.okayama-u.ac.jp (T. Suzuki).

0277-5387/$ - see front matter © 2009 Elsevier Ltd. All rights reserved.
doi:10.1016/j.poly.2009.04.010

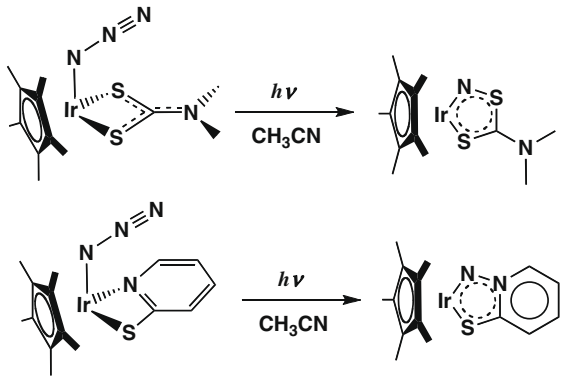

Scheme 1.

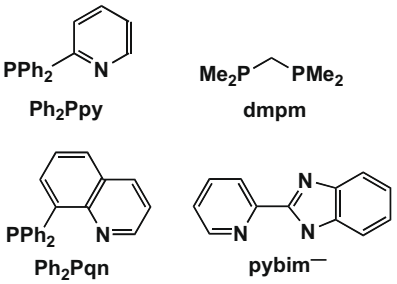

Scheme 2.

Caution! The AgN_3 resulting from the preparation of complex **2** is potentially explosive. Although we had no severe experience in our laboratory, all experiments handling the precipitated AgN_3 should be performed with the greatest care.

*2.1.1. [Cp*Ir(N$_3$)$_2$(Ph$_2$Ppy-κP)] (**1**)*

A methanol solution (6 cm^3) of Ph_2Ppy (135 mg, 0.57 mmol) was added with stirring to a solution of $[Cp^*Ir(N_3)_2]_2$ (236 mg, 0.287 mmol) in a mixture of dichloromethane and methanol (1:1, 4 cm^3), affording a yellow–brown precipitate in a few minutes. The reaction mixture was concentrated (to ca. 5 cm^3) under reduced pressure, and the resulting precipitate was collected by filtration. The crude product was washed with methanol (1 cm^3) and diethyl ether (3 cm^3), and recrystallized from a mixture of dichloromethane and methanol to give orange platelet crystals. Yield: 244 mg (63%). *Anal.* Calc. for $C_{27}H_{29}IrN_7P$: C, 48.06; H, 4.33; N, 14.53%. Found: C, 47.91; H, 4.28; N, 14.41%. ^1H NMR (CD_2Cl_2, 303 K): δ 1.44 (d, J_{HP} = 2.4 Hz, Cp*, 15H), 7.10–7.57 (m, Ph and py, 13H), 8.70 (dq, J_{HH} = 31.9 and 0.9 Hz, 6-py, 1H).

*2.1.2. [Cp*Ir(N$_3$)(Ph$_2$Ppy-κP,κN)]O$_3$SCF$_3$ (**2**)*

A methanol solution (3 cm^3) of $Ag(O_3SCF_3)$ (97 mg, 0.38 mmol) was added dropwise with stirring to an orange solution of **1** (255 mg, 0.378 mmol) in dichloromethane (2 cm^3). The mixture was stirred in the dark at room temperature for 18 h, and the resulting white precipitate (AgN_3) was filtered off. The precipitate was washed successively with acetonitrile (5 cm^3), methanol (5 cm^3) and dichloromethane (5 cm^3), and the filtrate and all washings were combined. The mixture was evaporated to dryness under reduced pressure, and the orange residue was dissolved in hot methanol (50 °C, 3 cm^3). After removal of undissolved impurities by filtration, the filtrate was allowed to stand in a refrigerator overnight, affording yellow–brown prismatic crystals. Yield: 226 mg (76%). *Anal.* Calc. for $C_{28}H_{29}F_3IrN_4O_3PS$: C, 43.02; H, 3.74; N, 7.17%. Found: C, 43.09; H, 3.79; N, 7.14%.

The corresponding PF_6 salt (**2′**) was prepared similarly using $AgPF_6$, instead of $Ag(O_3SCF_3)$.

*2.1.3. [Cp*Ir(N$_3$)(dmpm)]PF$_6$ (**3**)*

The ligand, dmpm (26 mg, 1.9 mmol) was added dropwise by syringe to a red suspension of $[Cp^*Ir(N_3)_2]_2$ (400 mg, 0.972 mmol) in methanol (10 cm^3) under a dinitrogen atmosphere. The reaction mixture was stirred at room temperature for 30 min and evaporated to dryness under reduced pressure. The residue was washed with Et_2O (10 cm^3 × 3), and then dissolved in methanol (2 cm^3) under air. A saturated methanol solution containing NH_4PF_6 (800 mg, 4.9 mmol) was added to the filtered methanol solution. The mixture was allowed to stand for 30 min to afford a pale yellow precipitate, which was collected by filtration, washed with methanol (1 cm^3) and Et_2O (3 cm^3), and dried in vacuo. The crude product was dissolved in a mixture of acetonitrile and methanol (1:1), and Et_2O vapor was diffused into the filtered solution to give yellow crystals of **3**. Yield: 432 mg (69%). *Anal.* Calc. for $C_{15}H_{29}F_6IrN_3P_3$: C, 27.69, H, 4.49; N, 6.46%. Found: C, 27.93; H, 4.47; N. 6.33%. ^1H NMR (CD_3CN, 303 K): δ 1.66 (virtual t, $^1J_{HP} + {}^3J_{HP}$ = 6.6 Hz, PMe, 6H), 1.83 (virtual t, $^1J_{HP} + {}^3J_{HP}$ = 6.2 Hz, PMe, 6H), 1.93 (s, Cp*, 15H), 3.49 (q, J_{HP} and J_{HH} = 15.9 Hz, CH_2, 1H), 4.68 (dt, J_{HP} = 15.6, J_{HH} = 10.5 Hz, CH_2, 1H).

*2.1.4. [Cp*Ir(N$_3$)(Ph$_2$Pqn)]PF$_6$ (**4**)*

Ph_2Pqn (74.8 mg, 0.239 mmol) was added to a suspension of $[Cp^*Ir(N_3)_2]_2$ (96.5 mg, 0.117 mmol) in methanol (5 cm^3), and the mixture was stirred at room temperature for 8 h. A methanol solution (3 cm^3) of NH_4PF_6 (137 mg, 0.839 mmol) was added to the resulting orange solution, affording an immediate precipitation. The precipitate was filtered off, washed with methanol (2 cm^3), and dried in vacuo. The crude product was recrystallized from acetonitrile/methanol to form orange platelet crystals. Yield: 171 mg (88%). *Anal.* Calc. for $C_{31}H_{31}F_6IrN_4P_2$: C, 44.98; H, 3.77; N, 6.77%. Found: C, 44.68; H, 3.93; N, 6.95%. ^1H NMR (CD_3CN, 303 K) δ 1.56 (d, J_{HP} = 2.4 Hz, Cp*).

*2.1.5. [Cp*Ir(pybim)(N$_3$)] (**5**)*

A methanol solution (3 cm^3) of Hpybim (46.7 mg, 0.239 mmol) and $NaOCH_3$ (13.8 mg, 0.255 mmol) was added to a suspension of $[Cp^*Ir(N_3)_2]_2$ (103.5 mg, 0.126 mmol) in a mixture of dichloromethane and methanol (2:1, 3 cm^3). The mixture was stirred at room temperature for 8 h and concentrated to ca. 1 cm^3 by a flow of dinitrogen. The resulting yellow precipitate was collected by filtration and dried in vacuo. Yield: 109.4 mg (77%). *Anal.* Calc. for $C_{22}H_{23}IrN_6$: C, 46.88; H, 4.11; N, 14.91%. Found: C, 46.50; H, 4.21; N, 14.88%. Yellowish orange platelet crystals suitable for the X-ray diffraction study were obtained from a mixture of dichloromethane and methanol.

2.2. Measurements

Proton NMR spectra were acquired on a JEOL EX270 or a Varian Mercury 300 spectrometer; chemical shifts were referenced to the residual ^1H NMR signals of the deuterated solvent and are reported versus TMS. Infrared spectra were measured on a JASCO FT/IR FT-550 spectrophotometer using Nujol mulls.

2.3. Crystallography

The X-ray diffraction data were obtained at −73(2) °C on a Rigaku R-axis rapid imaging plate detector with a graphite-monochromated Mo Kα radiation (λ = 0.71073 Å). A suitable crystal was mounted with a cryoloop and flash-cooled by cold dinitrogen stream. Data were processed by the Process-Auto program package [16a], and absorption corrections were made by the numerical

Table 1
Crystal data of complexes.

Compound	**1**	**2**	**3**	**4**·CH_3OH	**5**
Formula	$C_{27}H_{29}IrN_7P$	$C_{28}H_{29}F_3IrN_4O_3PS$	$C_{15}H_{29}F_6IrN_3P_3$	$C_{32}H_{35}F_6IrN_4OP_2$	$C_{22}H_{23}IrN_6$
FW	674.74	781.78	650.52	859.78	563.66
T/(K)	200(2)	200(2)	200(2)	200(2)	200(2)
Crystal system	monoclinic	monoclinic	monoclinic	monoclinic	monoclinic
Space group, *Z*	$P2_1/a$, 4	$P2_1/a$, 4	$P2_1/c$, 4	$P2_1/c$, 4	$P2_1/n$, 4
a/(Å)	17.5522(7)	10.0102(5)	8.7472(9)	8.6711(4)	8.2833(5)
b/(Å)	8.6997(4)	28.3235(12)	16.771(2)	14.3015(6)	16.2409(10)
c/(Å)	17.5992(8)	10.5269(5)	15.705(2)	26.485(1)	14.4564(9)
β/(°)	99.063(1)	96.222(2)	91.949(3)	93.975(1)	98.113(2)
V/(Å^3)	2653.8(2)	2967.0(2)	2302.7(5)	1843.3(13)	1925.3(2)
D_x/(Mg m^{-3})	1.689	1.750	1.876	1.743	1.945
μ(Mo Kα)/(mm^{-1})	5.135	4.680	6.061	4.240	6.957
T_{min}, T_{max}	0.427, 0.628	0.455, 0.604	0.377, 0.582	0.417, 0.484	0.337, 0.543
R_{int}	0.033	0.030	0.065	0.048	0.042
Reflection/parameter ratio	6056/331	4196/227	5182/263	7475/416	4398/268
R_1 [$F_o^2 > 2\sigma(F_o^2)$]	0.019	0.019	0.068	0.033	0.025
wR_2 (all reflection)	0.042	0.082	0.228	0.082	0.058
Goodness of fit	1.046	1.183	1.177	1.080	1.125

method from the crystal shapes [16b]. The structures were solved by the direct method using SIR2004 [17a], and refined on F^2 (with all independent reflections) using SHELXL97 [17b]. All non-H atoms were refined anisotropically, and H atoms were introduced at the positions calculated theoretically and treated with riding models. For the compound **3**, the positions of the F atoms of PF_6^- were severely disordered but no satisfactory model could be found. Therefore, the reported result was an artificially distorted structure for this anion. All calculations were carried out using the CRYSTAL STRUCTURE software package [16c].

Crystal data are collected in Table 1.

3. Results and discussion

3.1. 2-Diphenylphosphinopyridine (Ph_2Ppy) complexes

Kollipara et al. have recently reported the syntheses of $[Cp^*IrCl_2(Ph_2Ppy)]$, $[Cp^*IrCl(Ph_2Ppy)_2]PF_6$ and $[Cp^*IrCl(Ph_2Ppy)]PF_6$, as well as the crystal structures of the first two complexes having monodentately P-coordinated ligands (Ph_2Ppy-κP) [18]. Similar to their synthetic procedure and to the preparative method for $[Cp^*Ir(N_3)_2(napy\text{-}\kappa N)]$ (napy = 1,8-naphthyridine) [12], a stoichiometric reaction of $[Cp^*Ir(N_3)_2]_2$ and Ph_2Ppy (1:2 mole ratio) in a mixture of dichloromethane and methanol afforded an orange crystalline product of $[Cp^*Ir(N_3)_2(Ph_2Ppy)]$ (**1**) in 63% yield.

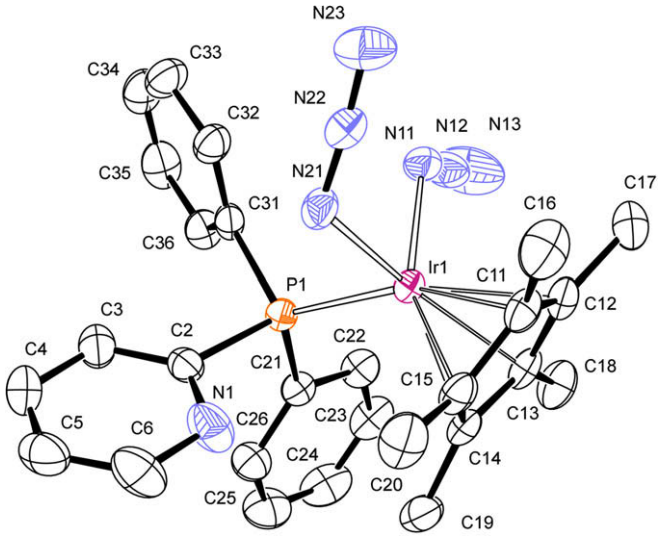

Fig. 1. An ORTEP view (50% probability level, hydrogen atoms omitted) of $[Cp^*Ir(N_3)_2(Ph_2Ppy\text{-}\kappa P)]$ (**1**).

The molecular structure of **1** determined by single-crystal X-ray analysis is illustrated in Fig. 1, which revealed the monodentate coordination mode of Ph_2Ppy through the P atom. In this analysis, three six-membered rings bound to the P atom, i.e., two phenyl and one pyridyl rings, were not distinguishable from one another, and the N atom of Ph_2Ppy could not be specified [19,20]. We tentatively assigned the N atom to the atom that was closest to Ir among the six possible atoms. Even under this assumption, the Ir1···N1 distance was 3.537(2) Å, which is far from being a bonding interaction. The structure of the "$Cp^*Ir(Ph_2Ppy)$" moiety in **1** is very similar to that in $[Cp^*IrCl_2(Ph_2Ppy\text{-}\kappa P)]$ [18]; the Ir–P bond lengths in **1** (2.3060(6) Å) and in the dichloro complex (2.299(2) Å) are comparable. Also, the "$Cp^*Ir(N_3)_2$" moiety corresponds well to that in $[Cp^*Ir(N_3)_2(napy\text{-}\kappa N)]$ [9]. The Ir–N(N_3) bonds in **1**, 2.112(3) and 2.129(2) Å, are comparable to those of the napy complex, 2.114(7) and 2.126(7) Å. The bending coordination mode and the intraligand structural parameters of the coordinated N_3^- ligands are also quite similar to those of the napy complex (see: Table 2).

The ligand, Ph_2Ppy, has the potential to form a four-membered chelate ring [21]. However, unlike the related bis(phosphino)methanes (dmpm or dppm; vide infra) and thiolates (2-Spy^- or 2-Sqn^-), a simple reaction of Ph_2Ppy with $[Cp^*Ir(N_3)_2]_2$ in a mixture of dichloromethane and methanol did not give the chelate complex. Kollipara et al. reported the formation of a chelate complex by the reaction of Ph_2Ppy and $[Cp^*IrCl_2]_2$ in methanol [18]. Here, to obtain a pure sample in high yield, we have utilized the reaction of complex **1** with a stoichiometric amount of $Ag(O_3SCF_3)$ or $AgPF_6$ for the preparation of $[Cp^*Ir(N_3)(Ph_2Ppy)](O_3SCF_3$ or $PF_6)$ (**2** or **2′**). The chelate coordination mode of Ph_2Ppy-$\kappa P,\kappa N$ was confirmed by X-ray analysis (Fig. 2). The Ir1–P1 bond length in **2** (2.3159(9) Å) is nearly the same as that in **1** (monodentately P-coordinated Ph_2Ppy complex). The Ir1–N1 bond length and the chelate bite angle of P1–Ir1–N1 in **2** are 2.125(3) Å and 67.40(8)°, respectively. These values are comparable to those in the corresponding 2-Spy complex (Ir–N = 2.111(4) Å, S–Ir–N = 67.0(1)°) [22] and 2-Sqn complex (Ir–N = 2.131(5) Å, S–Ir–N = 66.6(2)°) [7]. We expected, therefore, that the chelate Ph_2Ppy complex **2** would be stable, similar to the 2-Spy and 2-Sqn complexes. However, it was found that complex **2** was labile in acetonitrile solution.

Fig. 3 depicts the variable-temperature (−20–40 °C) ^1H NMR spectra of $[Cp^*Ir(N_3)(Ph_2Ppy)]PF_6$ (**2′**) in acetonitrile-d_3 (ca.

Table 2
Comparison of the structural parameters (Å, °) of the $Cp^*Ir^{III}(N_3)$ moiety and the vibration frequency, $\nu(N_3)$ (cm^{-1}).

Complex	Ir–C	Ir–N_α	Ir–N_α–N_β	N_α–N_β	N_α–N_β–N_γ	N_β–N_γ	$\nu(N_3)$
1	2.180(2)–2.223(2)	2.112(2)	118.7(2)	1.201(3)	176.7(3)	1.149(4)	2025
		2.129(2)	117.4(2)	1.198(3)	175.0(3)	1.153(3)	
2	2.171(3)–2.210(3)	2.108(3)	121.6(2)	1.202(4)	176.3(4)	1.151(5)	2036
3	2.170(12)–2.285(10)	2.113(13)	117.9(10)	1.230(17)	177.6(18)	1.155(18)	2035
4·CH_3OH	2.168(4)–2.244(4)	2.122(3)	120.5(3)	1.195(5)	175.8(5)	1.151(6)	2035
5	2.152(4)–2.186(3)	2.115(3)	124.3(3)	1.188(5)	174.4(4)	1.155(5)	2034
$[Cp^*Ir(N_3)_2(napy)]$	2.146(9)–2.185(8)	2.114(7)	124.5(6)	1.193(10)	176.4(9)	1.140(10)	2034
		2.126(7)	120.5(4)	1.180(10)	176.4(10)	1.170(10)	
$[Cp^*Ir(N_3)(bpy)]PF_6$	2.145(7)–2.179(7)	2.230(6)	116.4(6)	1.025(12)	172.3(10)	1.282(15)	2022
$[Cp^*Ir(Me_2dtc)(N_3)]$	2.159(7)–2.179(5)	2.120(6)	122.5(5)	1.197(8)	176.3(8)	1.157(9)	2030
$[Cp^*Ir(2\text{-}Sqn)(N_3)]$	2.144(6)–2.172(5)	2.132(6)	127.3(4)	1.178(7)	175.4(7)	1.127(7)	2035
	2.156(6)–2.174(6)	2.091(6)	124.2(5)	1.205(8)	175.3(7)	1.169(8)	
$[Cp^*Ir(8\text{-}Sqn)(N_3)]$	2.160(4)–2.197(4)	2.136(3)	120.5(3)	1.200(5)	175.9(5)	1.153(5)	2029
$[\{Cp^*Ir(N_3)\}_2(\mu\text{-}Hbimt)_2]$	2.155(5)–2.198(5)	2.109(4)	122.4(4)	1.181(6)	175.7(7)	1.158(7)	2036
	2.162(7)–2.202(7)	2.134(4)	118.1(4)	1.199(6)	176.3(6)	1.155(6)	2042[sh]

sh: Shoulder

0.05 mol dm^{-3}, prepared under a dinitrogen atmosphere). At 40 °C the Cp* resonance was observed as a broad signal around d 1.6. On cooling, this signal separated into two broad resonances with different intensities. At −20 °C both resonances were detected as sharp doublets at δ 1.51 and 1.64, with an intensity ratio of 4:1. The doublet resonances are indicative of the existence of an Ir–P bond, and, therefore, the two species in solution are assumed to be the chelate and the monodentately P-coordinated Ph_2Ppy complexes (Scheme 3). This results indicate that complex **2′** exists as an equilibrium mixture because of the dissociation of the Ir–N(py) bond in acetonitrile-d_3. Such a dissociation would be favorable for a N-atom insertion reaction, because the reaction of $[Cp^*Ir(N_3)(2\text{-}Spy)]$ was initiated by the photochemical cleavage of the Ir–N(py) bond [6]. However, photochemical or thermal reaction of an acetonitrile-d_3 solution of complex **2′** gave a complicated mixture of unidentified products, in which there was no lower-field shifted ^1H NMR resonance diagnostic for the two-legged piano stool structure of $Cp^*Ir^{III}(L\text{–}L')$-type complexes [5–7]. It has also been reported [23] that photolysis of $[Cp^*Ir(N_3)_2(PPh_3)]$ gave $[Cp^*Ir(H)(Ph_2PC_6H_4\text{-}\kappa P,\kappa C)]$, presumably via a "$Cp^*Ir^I(PPh_3)$" transient species formed by homoleptic cleavage of two Ir–$N(N_3)$ bonds. Thus, the present reactions might be caused by the undesirable thermal or photoreduction of the iridium(III) azido complex.

As mentioned above, the Ir–N(py) bond length and the chelate bite angle of complex **2** were comparable to those of $[Cp^*Ir(N_3)(2\text{-}Spy \text{ or } 2\text{-}Sqn)]$, while the solution behavior, i.e., the lability of the Ir–N(py) bond, was obviously different. To elucidate the reason for the different behavior from the structural point of view, we have also analyzed the crystal structures of the related complexes bearing dmpm and Ph_2Pqn.

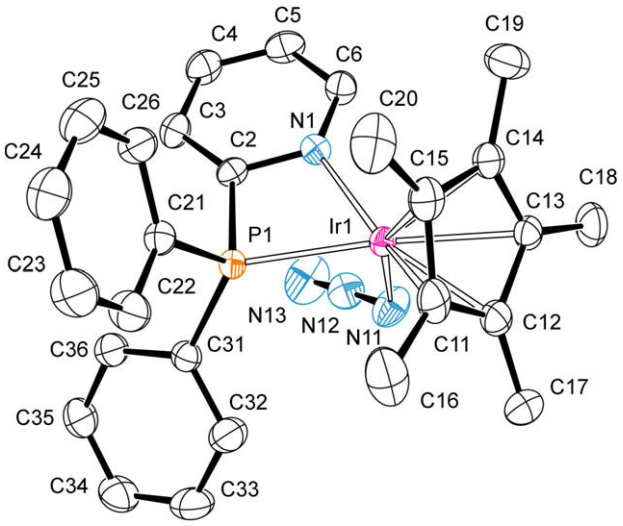

Fig. 2. An ORTEP view (50% probability level, hydrogen atoms omitted) of the cation in $[Cp^*Ir(N_3)(Ph_2Ppy\text{-}\kappa P,\kappa N)]O_3SCF_3$ (**2**).

3.2. Bis(dimethylphosphino)methane (dmpm) complex

It has been reported that particular Pt^{II}–dppm complexes of the form $[Pt(CH_2X)_2(dppm\text{-}\kappa^2P,P)]$ (X = Cl, Br, or I) demonstrated a fascinating chelate-ring expansion reaction by insertion of a CH_2

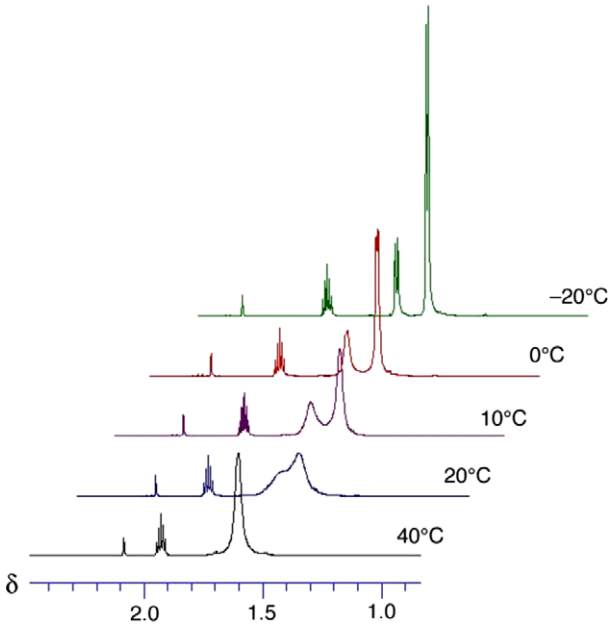

Fig. 3. Variable-temperature ^1H NMR spectra in the Cp* region of $[Cp^*Ir(N_3)(Ph_2Ppy\text{-}\kappa P,\kappa N)]PF_6$ (**2′**) in CD_3CN.

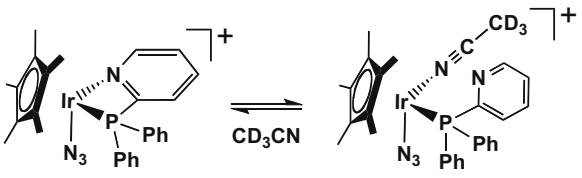

Scheme 3.

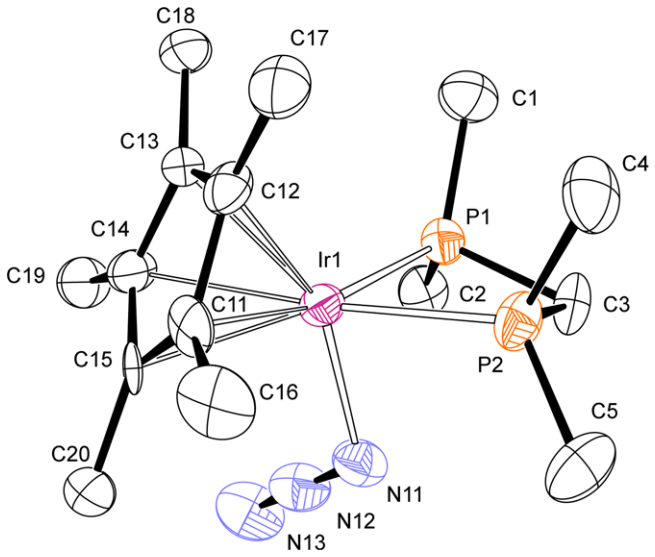

Fig. 4. An ORTEP view (50% probability level) of the cation in $[Cp^*Ir(N_3)(dmpm)]PF_6$ (**3**).

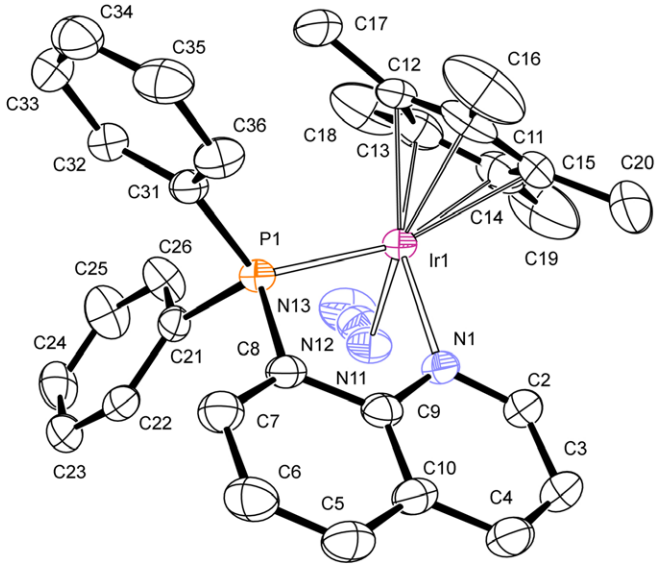

Fig. 5. An ORTEP view (50% probability level, hydrogen atoms omitted) of the cation in $[Cp^*Ir(N_3)(Ph_2Pqn)]PF_6{\cdot}CH_3OH$ (**4**·CH_3OH).

group into a Pt–P bond [24], which is somewhat related to a N-atom insertion reaction. Thus, we thought it might be interesting to investigate the structures and reactivities of the bis(phosphino)methane complexes of $[Cp^*Ir(N_3)(P–P)]PF_6$ (P–P = dppm or dmpm). These complexes were prepared in good yields by reaction of $[Cp^*Ir(N_3)_2]_2$ and the phosphines in methanol, followed by isolation of the PF_6 salts on addition of NH_4PF_6. We have also prepared the CF_3SO_3, BF_4 and BPh_4 salts of the dppm complexes, but none of them deposited suitable crystals for an X-ray diffraction study. Instead, we have determined the crystal structure of $[Cp^*Ir(N_3)(dmpm)]PF_6$ (**3**). The molecular structure with a four-membered chelate ring was confirmed, as illustrated in Fig. 4. The chelate bite angle, P1–Ir1–P2, of dmpm in complex **3** is 71.0(1)°, which is larger than those of Ph_2Ppy in complex **2**, 67.40(8)°. The Ir1–P1–C3 and Ir1–P2–C3 angles in **3** are 93.3(5) and 95.7(4)°, respectively, which are larger than the Ir1–P1–C2 angle in **2,** 85.9(1)°. These angular differences indicate clearly that the steric strain effects are more severe in the Ph_2Ppy chelate than in the dmpm chelate. It is also notable that two Ir–P bonds of complex **3** showed a large numerical deviation, Ir1–P1 2.344(4) versus Ir1–P2 2.282(3) Å, but we cannot account for this unusual feature at present.

Unlike the Ph_2Ppy chelate in complex **2**, the four-membered chelate rings in the dppm and dmpm complexes were stable in acetonitrile solution. When acetonitrile-d_3 solutions of the dppm and dmpm complexes were photolyzed by a high-pressure Hg lamp under a dinitrogen atmosphere at temperature below 0 °C, the ^1H NMR spectra of the resulting solutions indicated the formation of a complicated mixture of unidentified products. Similar to the case of Ph_2Ppy complex **2**, there was no lower-field shifted resonance diagnostic for Cp^*Ir^{III} complexes with a two legged piano stool structure. However, most of the Cp^* resonances became doublets (*cf.* the reactant complexes showed a triplet), because of coupling to the single P nucleus. This may suggest that a N-atom insertion could have taken place on photolysis.

3.3. 8-Diphenylphosphinoquinoline (Ph_2Pqn) complex

To clarify the structural features of the Ph_2Ppy chelate ring in complex **2**, the corresponding Ph_2Pqn complex was prepared and characterized by X-ray diffraction analysis for comparison. The complex, $[Cp^*Ir(N_3)(Ph_2Pqn)]PF_6$ (**4**), was obtained in nearly quantitative yield, and deposited orange prismatic crystals with a methanol molecule of crystallization, **4**·CH_3OH. The molecular structure of the cation in **4**·CH_3OH revealed by the X-ray diffraction study is shown in Fig. 5.

The chelate bite angle of Ph_2Pqn (P1–Ir1–N1) in complex **4** is 81.25(9)°, which is comparable to those in the other Ph_2Pqn complexes determined previously [21,25], but much larger than that of Ph_2Ppy in complex **2**, 67.40(8)°. The five-membered chelate ring is almost planar, and coplanar with the quinolyl ring. The deviations of atoms Ir1 and P1 from the least-square quinolyl ring plane are only 0.246(4) and 0.177(4) Å, respectively. The Ir1–P1–C8 angle in the chelate ring is 102.2(1)°, which is a little smaller than the ideal tetrahedral angle, but is normal for the coordinated phosphines. All bond angles around N1 are nearly 120°. These values indicate that the chelate coordination of Ph_2Pqn forms a strain-free planar five-membered ring. The Ir1–P1 and Ir1–N1 bond lengths in **4** are 2.294(1) and 2.115(3) Å, respectively, which are comparable to those in $[Cp^*Ir(8\text{-}Sqn)(N_3)]$ (Ir–N 2.104(3) Å), $[Cp^*IrCl(8\text{-}MeSqn)]PF_6$ (Ir–N 2.094(3) Å) [26], and the Ph_2Ppy complex **2** (vide supra). It is surprising that the Ir–P and Ir–N bonds in the highly strained four-membered Ph_2Ppy chelate ring elongate only by 0.02 and 0.01 Å, respectively, while the bond angles in the Ph_2Ppy ring show severe deviation from the ideal values: P–Ir–N 67.40(8)°, Ir–P–C 85.4(1)°, and Ir–N–C 106.3(2)°. This observation suggests that the primary reason for the dissociation of the Ir–N(py) bond of the Ph_2Ppy complex **2** in solution must be an angular strain in the four-membered chelate ring. In other words, even the bond lengths are seemingly comparable, the coordination bond in the strained chelate ring is remarkably weak and easy to dissociate in solution to relieve the steric strain.

In the crystal structure of **4**·CH_3OH, there was a stacking interaction between the quinolyl rings with a neighboring molecule, forming a dimer unit. The distance between the planes is ~3.6 Å. This stacking interaction is the most remarkable difference from the crystal structure of the Ph_2Ppy complex **2**.

3.4. 2-(2-Pyridyl)benzimidazolato (pybim) complex

In a series of studies we are investigating the molecular structures and photochemical reactivities of (azido)iridium(III) complexes containing various kinds of bidentate coligands, $[Cp^*Ir^{III}(N_3)(L–L')]^{+/0}$. Previously, we have reported the crystal

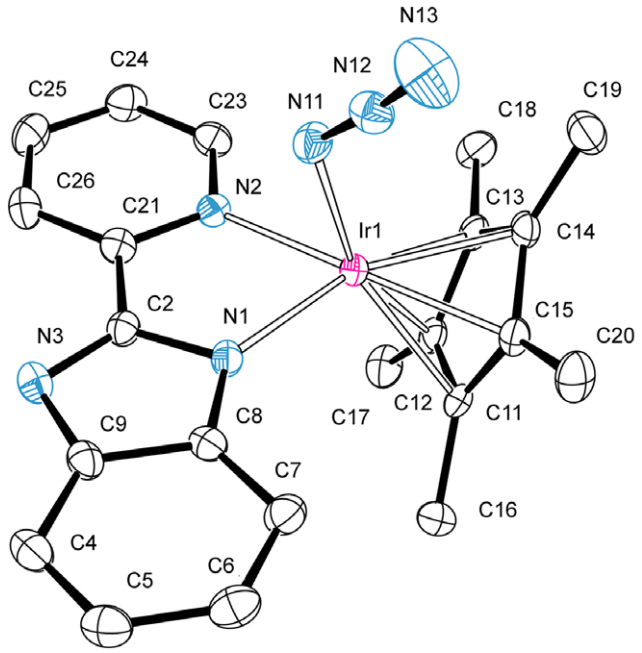

Fig. 6. An ORTEP view (50% probability level, hydrogen atoms omitted) of $[Cp^*Ir(N_3)_2(pybim)]$ (**5**).

structure of $[Cp^*Ir(N_3)(bpy)]PF_6$ [13], which showed an interesting 1,3-dipolar cycloaddition reaction in acetonitrile to form 5-methyltetrazolato complexes [20]. Furthermore, it has also been revealed that 2-pyridyl and 2-benzimidazolyl groups exhibited a different coordination behavior, at least when they were incorporated into bidentate thiolato ligands, i.e., 2-pyridinethiolate (2-Spy$^-$) and benzimidazole-2-thiolate (Hbimt$^-$) [7]. Thus, to compare directly the molecular structures between the bpy and pybim$^-$ complexes, we have prepared and characterized the pybim complex, $[Cp^*Ir(N_3)(pybim)]$ (**5**).

Complex **5** was obtained from $[Cp^*Ir(N_3)_2]_2$ and Na(pybim) as yellow–orange crystals in 77% yield. The molecular structure determined by X-ray analysis is shown in Fig. 6. As expected, the anionic pybim$^-$ ligand formed a planar five-membered chelate ring, which is coplanar with the pyridine and benzimidazolate rings. The chelate bite angle (N1–Ir1–N11) is 76.5(2)°, which is comparable to that of bpy in $[Cp^*Ir(N_3)(bpy)]PF_6$, 76.8(2)° [13]. The Ir1–N2(py) bond length in **5**, 2.139(3) Å, is longer than the Ir–N(bpy) bonds in the above bpy complex, 2.086(5) and 2.097(5) Å. The Ir–N1(bim) bond in **5** is 2.087(3) Å, which is remarkably shorter than the Ir1–N2(py) bond and comparable to the Ir–N(bim) bond length in a dinuclear 2-benzimidazolethiolato (Hbimt$^-$) complex of $[\{Cp^*Ir(N_3)\}_2(\mu\text{-Hbimt})_2]\cdot CH_3OH$, 2.098(4) Å [7]. Because the N ligator in the anionic benzimizadolate ring is more basic than that in the neutral pyridine ring, the bim-*N* donor would give a stronger σ-bonding interaction with an Ir^{III} center than the py-*N* does. When the bite angle of the ligands, N–E, are compared in $[Cp^*Ir^{III}(N_3)(N\text{–}E)]^{0/+}$ having a planar five-membered chelate ring, the angle increases in the order (N–E =) pybim$^-$ ≈ bpy < Ph_2Pqn < 8-Sqn$^-$. The same order was observed in the Ir–E bond lengths: Ir–N(pybim) 2.087(3) ≈ Ir–N(bpy) 2.092(7) < Ir–P(Ph_2Pqn) 2.294(1) < Ir–S (8-Sqn) 2.366(1) Å.

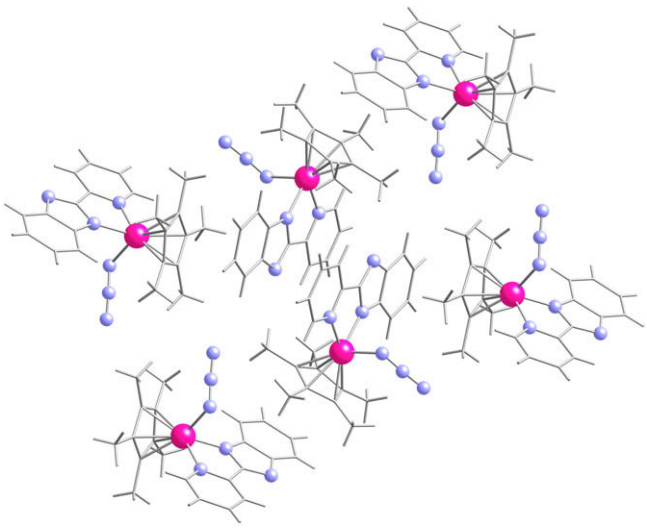

Fig. 7. A stacking diagram of the pybim complexes in the crystal.

The crystal structure of **5** exhibited a characteristic packing diagram. As seen in Fig. 7, a planar pybim ring is stacked with the other pybim ring in a neighboring molecule and a Cp* ring in another molecule. The interplanar distances between the planes are ~3.4 Å. In the crystal structure of $[Cp^*IrCl(Hpyim)]PF_6$ (Hpyim = 2-(2-pyridyl)imidazole) [9], a similar stacking interaction between a pair of Hpyim ligand planes was observed, in addition to the hydrogen-bonding interaction between the im-H group and the coordinated Cl$^-$ ligand. However, in the present complex **5** the N3 atom of the pybim ligand was free from coordination or hydrogen-bonding interaction.

3.5. Comparison of the structural parameters of the $Cp^*Ir^{III}(N_3)$ moiety

The structural parameters of the $Cp^*Ir^{III}(N_3)$ moiety in the complexes determined in the previous and present studies are collected in Table 2. The Ir–C bond lengths of the complexes analyzed previously were in the range of 2.14–2.20 Å. However, some of the Ir–C bonds in complexes **1**–**4** are slightly longer than 2.20 Å (up to 2.29 Å). A detailed examination revealed that the elongated Ir–C bonds are all *trans* to the phosphino donor group(s). Thus, it is concluded that the Ir–C bonds of the Cp* group are also affected by the strong *trans* influence of the phosphines.

The parameters associated with the Ir–N_3 moiety are very similar among the complexes listed in Table 2, except for the bpy complex of $[Cp^*Ir(N_3)(bpy)]PF_6$. Namely, in most (azido)iridium(III) complexes the Ir–N_α bond lengths are in the range 2.09–2.14 Å and the Ir–N_α–N_β bond angles are in the range 117–127°. The coordinated azido ligands are nearly linear (N_α–N_β–N_γ 174–177°), with longer N_α–N_β (1.18–1.23 Å) bonds than N_β–N_γ (1.13–1.17 Å) bonds. In contrast, in $[Cp^*Ir(N_3)(bpy)]PF_6$ all of the parameters for the Ir–N_3 moiety are outside the above ranges. In particular, the Ir–N_α bond is strikingly long at 2.230(6) Å, and the N_α–N_β bond (1.025(12) Å) is remarkably shorter than the N_β–N_γ bond (1.282(15) Å). Consistent with the differences in these structural parameters, the $\nu(N_3)$ stretching frequency of the bpy complex, 2022 cm^{-1}, is observed at a slightly lower frequency than those of the other complexes (Table 2). At this time, we cannot explain these exceptional observation for the bpy complex, but they could give an important insight into the different reactivity of the bpy complex from the others [25].

4. Conclusion

In this study, the crystal structures of five (azido)iridium(III) complexes bearing potentially bidentate ligands (L–L′) have been determined and their structural parameters have been discussed, together with those of the related complexes analyzed previously. Comparing the parameters of the four-membered chelate ring

formed by Ph_2Ppy (in complex **2**) with those of the five-membered chelate ring of the related phosphine–imine-type hybrid ligand Ph_2Pqn (in complex **4**), it became apparent that the Ph_2Ppy ring was highly strained as indicated by the smaller bond angles, but the Ir–P/N coordination bond lengths were comparable to those in the strain-free Ph_2Pqn chelate ring. Although the Ir–N bond and the Ir–N–C angle in the Ph_2Ppy complex **2** are similar to those in the 2-Spy and 2-Sqn complexes analyzed previously [6,22], complex **2** exhibits a dissociation equilibrium of the Ir–N(py) bond in acetonitrile solution.

The pybim complex showed an interesting molecular and crystal structure. The ligand, $pybim^-$, forms a planar five-membered chelate ring with an extended π-delocalized system, and the pybim plane shows a stacking interaction with the neighboring pybim and Cp^* planes to give a characteristic packing structure of the crystal. Furthermore, the Ir–N(bim) bond is shorter than the Ir–N(py) bond, because of the stronger electron-donating properties of the benzimidazole moiety.

We have also examined the photochemical and thermal reactivities of the complexes described in this study, but they showed a complicated mixture of unidentified products.

Supplementary data

CCDC 711474, 711475, 711476, 711477, and 711478 contain the supplementary crystallographic data for **1, 2**, **3**, **4**·CH_3OH, and **5**, respectively. These data can be obtained free of charge via http://www.ccdc.cam.ac.uk/conts/retrieving.html, or from the Cambridge Crystallographic Data Centre, 12 Union Road, Cambridge CB2 1EZ, UK; fax: (+44) 1223-336-033; or e-mail: deposit@ccdc.cam.ac.uk.

Acknowledgement

This work was supported by Grant-in-Aid for Scientific Research No. 20550064 from the Ministry of Education, Culture, Sports, Science, and Technology, Japan.

References

[1] J. Šima, Coord. Chem. Rev. 250 (2006) 2325.
[2] (a) J.F. Berry, E. Bill, E. Bothe, S.D. George, B. Mienert, F. Neese, K. Wieghardt, Science 312 (2006) 1937;
(b) J. Du Bois, C.S. Tomooka, J. Hong, M.E. Carreira, Acc. Chem. Res. 30 (1997) 364.
[3] (a) H.C. Kolb, M.G. Finn, K.B. Sharpless, Angew. Chem., Int. Ed. 40 (2001) 2004;
(b) M. Obata, A. Kitamura, A. Mori, C. Kameyama, J.A. Czaplewska, R. Tanaka, I. Kinoshita, T. Kusumoto, H. Hashimoto, M. Harada, Y. Mikata, T. Funabiki, S. Yano, Dalton Trans. (2008) 3292;
(c) S. Mukhopadhyay, J. Lasri, M.A.J. Charmier, M.F.C. Guedes da Silva, A.J.L. Pombeiro, Dalton Trans. (2007) 5297.
[4] (a) H.-B. Xu, B.-W. Wang, F. Pan, Z.-M. Wang, S. Gao, Angew. Chem., Int. Ed. 46 (2007) 7388;
(b) T.-F. Liu, D. Fu, S. Gao, Y.-Z. Zhang, H.-L. Sun, G. Su, Y.-J. Liu, J. Am. Chem. Soc. 125 (2003) 13976;
(c) J. Carranza, C. Brennan, J. Sletten, J.M. Clemente-Juan, F. Lloret, M. Julve, Inorg. Chem. 43 (2003) 8716;
(d) M. Habib, T.K. Marmakar, G. Aromi, J. Ribas-Ariño, H.-K. Fun, S. Chantrapromma, S.K. Chandra, Inorg. Chem. 47 (2008) 4109.
[5] T. Suzuki, A.G. Dipasquale, J.M. Mayer, J. Am. Chem. Soc. 125 (2003) 10514.
[6] Y. Sekioka, S. Kaizaki, J.M. Mayer, T. Suzuki, Inorg. Chem. 44 (2006) 8173.
[7] M. Kotera, Y. Sekioka, T. Suzuki, Inorg. Chim. Acta 361 (2008) 1479.
[8] (a) V. Pons, D.M. Heinekey, J. Am. Chem. Soc. 125 (2003) 8428;
(b) K.-I. Fujita, M. Nakamura, R. Yamaguchi, Organometallics 20 (2001) 100.
[9] K. Pachhunga, B. Therrien, K.A. Kreisel, G.P.A. Yap, M.R. Kollipara, Polyhedron 26 (2007) 3638.
[10] M. Albrecht, T. Scheiring, T. Sixt, W. Kaim, J. Organomet. Chem. 596 (2000) 84.
[11] K. Yamanari, R. Ito, S. Yamamoto, T. Konno, A. Fuyuhiro, M. Kobayashi, R. Arakawa, Dalton Trans. (2003) 380.
[12] T. Suzuki, Inorg. Chim. Acta 359 (2006) 2431.
[13] T. Suzuki, Acta Crystallogr., Sect. E 61 (2005) m488.
[14] A. Maisonnet, J.P. Farr, M.M. Olmstead, C.T. Hunt, A.L. Balch, Inorg. Chem. 21 (1982) 3961.
[15] R.D. Feltham, H.G. Metzer, J. Organomet. Chem. 33 (1971) 347.
[16] (a) PROCESS-AUTO, Automatic Data Acquisition and Processing Package for Imaging Plate Diffractometer, Rigaku Corporation, Akishima, Tokyo, Japan, 1998.;
(b) T. Higashi, SHAPE, Program to obtain Crystal Shape using CCD Camera, Rigaku Corporation, Tokyo, Japan, 1999.;
(c) CRYSTAL STRUCTURE Ver. 3.6.0, Crystal Structure Analysis Package, Rigaku and Rigaku/MSC, Akishima, Tokyo, Japan and The Woodlands, TX, USA, 2000–2004.
[17] (a) M.C. Burla, R. Caliandro, M. Camalli, B. Carrozzini, G.L. Cascarano, L. De Caro, C. Giacovazzo, G. Polidori, R. Spagna, SIR2004, 2005.;
(b) G.M. Sheldrich, SHELXL97, University of Göttingen, Göttingen, Germany, 1997.
[18] P. Covindaswamy, P. Carroll, Y.A. Mozharivskyj, M.R. Kollipara, J. Chem. Sci. 118 (2006) 319.
[19] M. Kotera, Y. Sekioka, T. Suzuki, Inorg. Chem. 47 (2008) 3498.
[20] M. Rashidi, K. Kamali, M.C. Jennings, R.J. Puddephatt, J. Organomet. Chem. 690 (2005) 1600.
[21] T. Suzuki, T. Kuchiyama, S. Kishi, S. Kaizaki, M. Kato, Bull. Chem. Soc. Jpn. 75 (2002) 2433.
[22] Y. Sekioka, T. Suzuki, Bull. Chem. Soc. Jpn. 79 (2006) 1897.
[23] D.A. Freedman, K.R. Mann, Inorg. Chem. 30 (1991) 836.
[24] N.W. Alcock, P.G. Pringle, P. Bergamini, S. Sostero, O. Traverso, J. Chem. Soc., Dalton Trans. (1990) 1553.
[25] T. Suzuki, Bull. Chem. Soc. Jpn. 77 (2004) 1869.
[26] S. Ye, W. Kaim, M. Albrecht, F. Lissner, T. Schleid, Inorg. Chim. Acta 357 (2004) 3325.